

Nd *L*-shell x-ray emission induced by light ions

Xian-Ming Zhou(周贤明), Jing Wei(尉静), Rui Cheng(程锐), Yan-Hong Chen(陈燕红),Ce-Xiang Mei(梅策香), Li-Xia Zeng(曾利霞), Yu Liu(柳钰), Yan-Ning Zhang(张艳宁), Chang-Hui Liang(梁昌慧), Yong-Tao Zhao(赵永涛), and Xiao-An Zhang(张小安)

Citation: Chin. Phys. B, 2022, 31 (**6**): 063204. DOI: 10.1088/1674-1056/ac4488
Journal homepage: http://cpb.iphy.ac.cn; http://iopscience.iop.org/cpb

What follows is a list of articles you may be interested in

X-ray emission for Ar^{11+} ions impacting on various targets in the collisions near the Bohr velocity

Xian-Ming Zhou(周贤明), Jing Wei(尉静), Rui Cheng(程锐), Yan-Hong Chen(陈燕红), Ce-Xiang Mei(梅策香), Li-Xia Zeng(曾利霞), Chang-Hui Liang(梁昌慧), Yao-Zong Li(李耀宗), Yong-Tao Zhao(赵永涛), and Xiao-An Zhang(张小安)

Chin. Phys. B, 2021, 30 (**8**): 083201. DOI: 10.1088/1674-1056/abe22f

Imprint of transient electron localization in H_2^+ using circularly-polarized laser pulse

Jianghua Luo(罗江华), Jun Li(李军), and Huafeng Zhang(张华峰)

Chin. Phys. B, 2020, 29 (**12**): 123201. DOI: 10.1088/1674-1056/abbbe1

Charge-state populations for the neon-XFEL system

Ping Deng(邓萍), Gang Jiang(蒋刚)

Chin. Phys. B, 2019, 28 (**6**): 063203. DOI: 10.1088/1674-1056/28/6/063203

Extreme ultraviolet and soft x-ray spectral lines in Rb XXIX

Indu Khatri, Arun Goyal, Sunny Aggarwal, A K Singh, Man Mohan

Chin. Phys. B, 2016, 25 (**3**): 033201. DOI: 10.1088/1674-1056/25/3/033201

Broadband time-resolved elliptical crystal spectrometer for X-ray spectroscopic measurements in laser-produced plasmas

Wang Rui-Rong, Jia Guo, Fang Zhi-Heng, Wang Wei, Meng Xiang-Fu, Xie Zhi-Yong, Zhang Fan

Chin. Phys. B, 2014, 23 (**11**): 113201. DOI: 10.1088/1674-1056/23/11/113201

Nd *L*-shell x-ray emission induced by light ions

Xian-Ming Zhou(周贤明)[1,2,†], Jing Wei(尉静)[1], Rui Cheng(程锐)[3], Yan-Hong Chen(陈燕红)[3], Ce-Xiang Mei(梅策香)[1], Li-Xia Zeng(曾利霞)[1], Yu Liu(柳钰)[1], Yan-Ning Zhang(张艳宁)[1], Chang-Hui Liang(梁昌慧)[1], Yong-Tao Zhao(赵永涛)[2,3], and Xiao-An Zhang(张小安)[1,3]

[1] *Ion Beam and Optical Physics Joint Laboratory of Xianyang Normal University and Insitite of Modern Physics, Chinese Academy of Sciences, Xianyang Normal University, Xianyang* 712000, *China*

[2] *School of Science, Xi'an Jiaotong University, Xi'an* 710049, *China*

[3] *Institute of Modern Physics, Chinese Academy of Sciences, Lanzhou* 730000, *China*

(Received 27 September 2021; revised manuscript received 15 December 2021; accepted manuscript online 18 December 2021)

The *L*-shell x-ray of Nd has been obtained for 300–600 keV He^{2+} ions impacting, and compared with that produced by H^+ and H_2^+ ions. The threshold of projectile kinetic energy for *L*-shell ionization of Nd is crudely verified in the energy region of about 300–400 keV. It is found that the energy of the distinct *L*-subshell x-rays has a blue shift. The relative intensity ratios of $L\beta_{1,3,4}$ and $L\beta_{2,15}$ to $L\alpha_{1,2}$ x-ray are enlarged compared to the atomic data, and they decrease with the increase of the incident energy, and increase with increasing the effective nuclear charge of the incident ions. That is interpreted by the multiple ionization of outer-shells induced by light ions.

Keywords: light ions, ion–atom collision, *L*-shell x-ray, multiple ionization

PACS: 79.20.Rf, 32.80.Aa, 32.30.Rj, 32.80.Rm **DOI:** 10.1088/1674-1056/ac4488

1. Introduction

The ion–atom collisions have been extensively investigated experimentally and theoretically in the past few decades to meet the requirement of fundamental research and practical applications.[1–8] During such collisions, the inner-shell electrons of projectile and target atom can be excited by the direct Coulomb ionization or charge transfer. The corresponding vacancy decays radiatively by x-ray emission or nonradiatively by Auger or Coster–Kronig (CK) transition processes. The parameters of the x-ray, such as, emission energy, line width, satellite structure and production cross section, can provide significant information for the atomic structure, inner-shell process in collisions, plasma characteristic, and so on. Therefore, the x-ray emission studies are not only an important method for the experimental research on atomic collision mechanism and verification of the relative theory, but also has important significance for many basic research, for instance, the technique of particle induced x-ray emission (PIXE), diagnosis of dense plasma and laboratory astrophysics.[9–12]

Multiple ionization state, which means more than one outer-shell electrons are absent at the moment of inner-shell x-ray emission, can be produced by the subsequent Auger transition and CK transition or simultaneous direct ejection of several electrons with relatively high probability in collisions of ion-atom by the strong Coulomb field of the projectile.[13,14] This action results in a reduction of the nuclear charge screening, and thus increases the binding energy of the residual orbital electrons, and alters the fluorescence yield of radiative transition. Consequently, the x-ray energy shifts to the high energy side, with respect to the data of singly ionized atom, and the relative intensity ratio of the subshell x-rays is changed. Generally, such phenomena can be caused by swift highly charged heavy ions.[15–17] However, a few recent experimental results demonstrate that the multiple ionization can also be induced by low-energy light ions.[18–20] In our previous work, such phenomena by low-energy protons and the dependence on the proton energy has been investigated.[21] Here, we would like to present further research on the multiple ionization for He^{2+} and H_2^+ ions impacting.

In the present work, the measurement of the *L*-shell x-ray of neodymium (Nd) is presented for He^{2+} ions in the energy region of 300–600 keV, and H^+ and H_2^+ ions with energy of about 150 keV/u. The threshold of incident energy for Nd *L*-shell x-ray emission is checked. The line energy and relative intensity ratio of the *L*-subshell x-rays are analyzed as a function of the projectile energy and effective nuclear charge. The multiple ionization induced by low energy light ions is discussed.

2. Experimental method

The measurements have been carried out at 320 kV high voltage experimental platform at the Institute of Modern Physics, Chinese Academy of Sciences (IMP, CAS) in Lanzhou, China. More details of the experimental system have been described in a previous work.[22] The experimental setup is shown in Fig. 1. In brief, the He^{2+}, H_2^+ and H^+ ions are produced and extracted from the electron cyclotron resonance (ECR) ion source and selected by a 90° analyzing magnet,

†Corresponding author. E-mail: xmzhou19860208@163.com

© 2022 Chinese Physical Society and IOP Publishing Ltd

and then introduced into the ultrahigh vacuum target chamber (10^{-8} mbar) after acceleration, focus, multi-deflections and multi-collimations. The divergence of the beam is smaller than 0.2°. The ion beam impacts perpendicularly onto the target with a spot size of about Φ3 mm. The number of incident projectiles, which could not be measured immediately by recording the target current due to the influence of the secondary electron emission, is detected indirectly by the combined use of a penetrable Faraday cup and a common one.

The emitted x-rays are detected by a silicon drift detector (SDD) produced by AMPTEK. The SDD has an effective detection area of 7 mm^2 and a 12.5 μm Be window in the front of the detector. The SDD is placed at 80 mm far away from the target surface in the chamber and at 135° angle with respect to the beam direction. The detector has an effective energy range of 0.5–14.3 keV when the gain was selected at 100, and an energy resolution of about 136 eV at 5.9 keV. The energy calibration is done by using simultaneously two standard radioactive sources of ^{55}Fe and ^{241}Am, and then tested by measuring the energies of the K-shell x-ray of Al, V and Fe induced by photon irradiation, which is produced by a Mini-X x-ray tube and has an energy of about 5–40 keV. In this way, a precise measurement for the x-ray energy can be guaranteed. The SDD intrinsic efficiency, which combines the transmission effect through the Be window and the interaction in the silicon detector, is well determined by the transmission measurement.

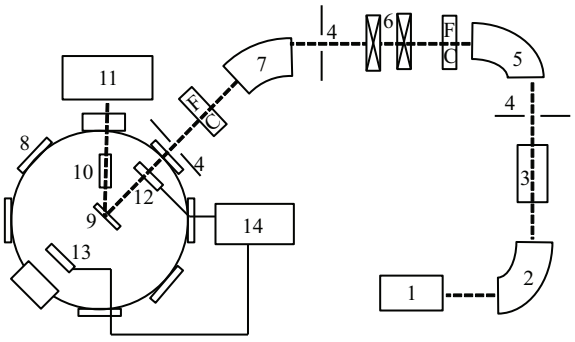


Fig. 1. Schematic drawing of experiment setup: 1, ECR ion source, 2, analyzing magnet, 3, high volt accelerate platform, 4, barrier, 5, 90° deflection magnet, 6, magnetic quadrupled lens, 7, 60° deflection magnet, 8, ultrahigh vacuum target chamber, 9, target, 10, silicon drift detector, 11, x-ray recording system, 12, penetrable faraday cup, 13, common faraday cup, 14, projectile number recording system.

3. Results and discussion

3.1. Kinetic energy threshold of Nd L-shell x-ray emission

In the present work, the incident energy of He^{2+} ions is 300–600 keV with interval of 100 keV. The Nd L-shell x-rays are observed at all incident energies except at 300 keV. As shown in Fig. 2, six distinct lines are observed and identified as $L\iota$, $L\alpha_{1,2}$, $L\beta_{1,3,4}$, $L\beta_{2,15}$, $L\gamma_1$ and $L\gamma_{2,3,4,4'}$ x-ray, which are emitted from the radiative decay of L-subshell vacancies.[23,24] The corresponding vacancy is a prerequisite for the x-ray emission. So, it is proposed that there is a kinetic energy threshold for the ionization of L-shell electrons between 300 keV and 400 keV.

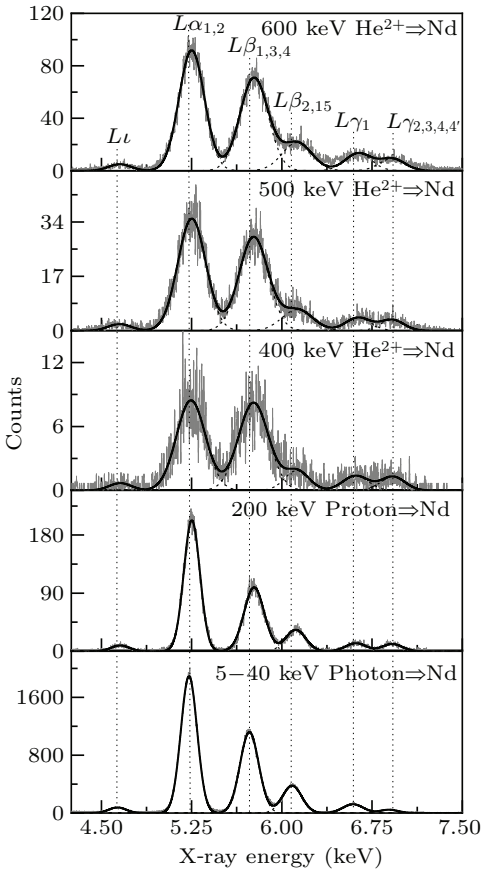


Fig. 2. Typical L x-ray spectra of neodymium induced by He^{2+} ions, and compared with that by proton and photon.

The inner-shell process induced by ion-atom collision can be simulated by the binary encounter approximation (BEA) model.[25] Here, the ionized orbital electrons of target atom can be regarded as free electrons, and the ionization is described as the classical Coulomb collision between the projectile and the expelled electron. The momentum and kinetic energy are conserved. For a crude estimation, it is assumed that, at the minimum mean collision distance, the Coulomb potential between the projectile and the ionized electron must be at least greater than or equal to the binding energy of the ionized electron, if the inner-shell electrons are to be ionized. Therefore, the kinetic energy threshold for producing holes in the inner shell of the target atom can be estimated as[26–28]

$$E_{\rm th} = \frac{z_1' z_2'}{q} \cdot \frac{M_1 + M_2}{M_2} \cdot U_{\rm i}, \tag{1}$$

where z_1' (z_2') and M_1 (M_2) are the effective nuclear charge and mass number of projectile (target atom). q is the charge state of incident ions. $U_{\rm i}$ is the binding energy of the ionized orbital electron. For He^{2+}, the value of z_1' is equal to that of q. $z_2' = z_2 - \delta$, where δ is the atomic screening constant, and can be derived from the analysis of optimized orbital exponents on the computation of self-consistent-field method.[29,30]

For Nd, the average binding energy of 2s and 2p electrons are about 7126 eV and 6465 eV. Based on Eq. (1), the kinetic energy threshold for the ionization of 2s and 2p electrons are predicted as 322 keV and 375 keV, respectively. This is in agreement with the experimental results. At the incident energy of 400 keV, the *L*-shell x-rays of Nd are observed, but they are not observed at 300 keV.

3.2. Energy shift of the *L*-subshell x-ray

In Fig. 2, the typical x-ray emission spectra of Nd produced by He^{2+} ions are presented as a function of incident energy, and compared with that of lower energy proton and photon. The spectra can be well fitted by a nonlinear curve Gaussian program. One can find that the energy of the spectral lines produced by He^{2+} ions are similar to the result of proton, and have a blue shift toward the high energy direction than that of photon, which can be considered as a standard atomic spectrum. For example, the measured energies of the six *L*-subshell x-rays are listed in Table 1. There is no obvious regular change with the increase of kinetic energy, and they are almost constant within the estimated error range, but larger than that of a singly ionized atom and that of photon, which is nearly the same as the atomic data apart from $L\gamma_1$. This is consistent with the result of lower energy proton.[21]

Table 1. Energies of Nd *L*-subshell x-ray induced by He^{2+} ions. For comparison, the data of the singly ionized atom (DSIA) and that produced by 5–40 keV photon and 200 keV protons were also given.[23,24,31]

	$L\iota$ (eV)	$L\alpha_{1,2}$ (eV)	$L\beta_{1,3,4}$ (eV)	$L\beta_{2,15}$ (eV)	$L\gamma_1$ (eV)	$L\gamma_{2,3,4,4'}$ (eV)
400 keV He^{2+}	$4657_{\pm3}$	$5245_{\pm3}$	$5765_{\pm5}$	$6124_{\pm7}$	$6627_{\pm7}$	$6922_{\pm7}$
500 keV He^{2+}	$4651_{\pm3}$	$5252_{\pm3}$	$5765_{\pm5}$	$6129_{\pm7}$	$6635_{\pm7}$	$6916_{\pm7}$
600 keV He^{2+}	$4653_{\pm3}$	$5251_{\pm3}$	$5769_{\pm5}$	$6126_{\pm7}$	$6635_{\pm7}$	$6916_{\pm7}$
Proton[31]	$4659_{\pm3}$	$5252_{\pm3}$	$5764_{\pm5}$	$6124_{\pm3}$	$6619_{\pm5}$	$6913_{\pm5}$
Photon[31]	$4633_{\pm3}$	$5228_{\pm3}$	$5727_{\pm5}$	$6090_{\pm3}$	$6592_{\pm5}$	$6893_{\pm5}$
DSIA[23,24]	4633	5228	5726	6090	6604	6894

In the previous work, we have investigated the multiple ionization induced by lower energy proton and the dependence on the incident energy by analyzing the *L*-subshell x-ray emission. In the energy range of 100–250 keV/u, the outer-shell electrons of medium *Z* elements, such as *M*, *N*, and *O*, can be multiply ionized by the bombardment of light ions, and the extent of such multiple ionization decreases with the increase of incident energy. It is proposed that the same is anticipated for He^{2+} ions. Here, the observed blue shift mainly results from outer-shell multiple ionization of Nd by the He^{2+} impacting, and that presents a dwindling trend as a function of the incident energy. And it can also be verified in the following discussion of the relative intensity ratio. However, due to the limitation of the detector's energy resolution, no obvious distinction of the experimental blue shift is obtained for various projectile' energy.

3.3. Relative intensity ratio of the *L*-subshell x-ray

In addition to the blue shift of energy, multiple ionization of outer shell can cause changes in the x-ray fluorescence yield, because the probability of radiationless transition is altered due to the absence of electrons in outershells. This will result in a change in the relative intensity ratio of the *L*-subshell x-rays. It can be seen from Fig. 2 that although the spectral shapes at different incident energies are relatively similar, there is a significant decrease in the $L\beta_{1,3,4}$ x-ray emissions with increasing incident energy, compared to that of $L\alpha_{1,2}$ x-ray. For further quantitative analysis, the relative intensity ratios of $L\beta_{1,3,4}$ and $L\beta_{2,15}$ to $L\alpha_{1,2}$x rays are investigated. As shown in Figs. 3 and 4, the ratio is higher than the atomic data and that of photon and proton, and is dwindled as the incident energy increases. This provides another credible evidence for the outer-shell multiple ionization of target atom by impact of lower energy light ions.

The $L\beta_{1,3,4}$ x-ray consists of three lines, which come from the radiation transitions of M_4–L_2, M_3–L_1 and M_2–L_1, respectively. $L\beta_1$ and $L\alpha_{1,2}$ x-ray mainly originate from the transitions of 3d electrons to L_2 and L_3 vacancy, and the corresponding fluorescence yield are 0.031 and 0.058 for Nd. The Auger yield a_2 and a_3 for the decay of L_2 and L_3 vacancy are 0.724 and 0.875.[32,33] They are not much different in the same magnitude. When the outer shells are multiply ionized, the drop in Auger yield should be at the same extent, and the resulting enlargement in the fluorescence yield should also be of the same magnitude. This will not result in an obvious change in the relative intensity ratio of $L\beta_{1,3,4}$ to $L\alpha_{1,2}$ x-rays.

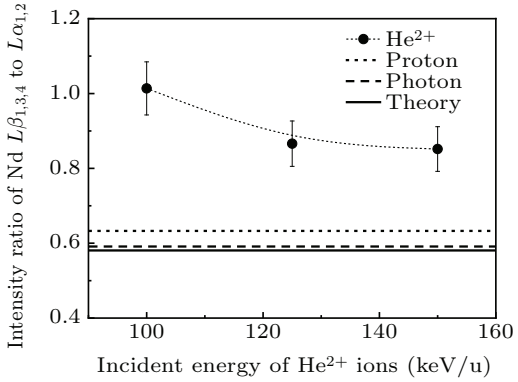


Fig. 3. Relative intensity ratios of Nd $L\beta_{1,3,4}$ to $L\alpha_{1,2}$ x-ray for He^{2+} ions impact as a function of the incident energy, and the data for 200 keV proton, 5–40 keV photon, and the theoretical calculation for the singly ionized atom.

However, there is an additional channel of CK transition for the decay of L_2 vacancy compared with that of L_3. In the case of multiple ionization, the Coster–Kronig yield f_{23} is diminished. Correspondingly, the probability of radiation transition, namely, the fluorescence yield of $L\beta_1$ x-ray, will increase. Moreover, owing to the absence of some outer-shell electrons, some of the non-radiative transition is restricted for the de-excitation of L_1 vacancy, and the fluorescence yield ω_1 increases. This will result in an enhancement of the $L\beta_{3,4}$ x-ray emission. In summary, the experimental relative intensity ratio of $L\beta_{1,3,4}$ to $L\alpha_{1,2}$ x-ray is enlarged as shown in Fig. 3, and decreases with increasing incident energy as the dawdle of the multi-ionization degree.

The $L\beta_{2,15}$ and $L\alpha_{1,2}$ x-rays are mainly the result of radiation de-excitation of L_3 vacancy filled by N and M electrons, respectively. When multiple electrons are missing in the outer shell, the Auger transition filling the L_3 vacancy is suppressed, and the corresponding radiation transition is enhanced, because the sum of fluorescence yield ω_3 and Auger yield a_3 is unity. The Auger yield a_3 of Nd is almost 9 and 46 times higher than the fluorescence yield of $L\alpha_{1,2}$ and $L\beta_{2,15}$ x-ray.[32,33] The fluorescence yield of $L\beta_{2,15}$ x-ray is more susceptible to the effect of multiple ionization. As a result, the $L\beta_{2,15}$ x-ray emission has a larger enhancement than that of $L\alpha_{1,2}$. The relative intensity ratio of $L\beta_{2,15}$ to $L\alpha_{1,2}$ x-ray is higher than the atomic data as shown in Fig. 4.

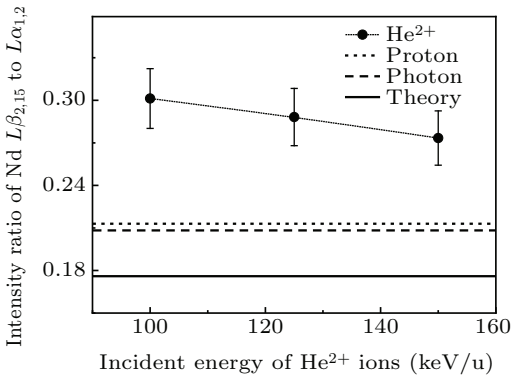


Fig. 4. Relative intensity ratios of Nd $L\beta_{2,15}$ to $L\alpha_{1,2}$ x-ray for He^{2+} ions impact as a function of incident energy, and the data for 200 keV proton, 5–40 keV photon, and the theoretical calculation for the singly ionized atom.

3.4. Dependence of multiple ionization on the effective nuclear charge

In a simple approach based on the independent-particle framework, the electron correlation effect is not taken into account, and the multiple ionization can be treated as simultaneous independent single ionization of the orbital electrons. The probability of multiple ionization can be estimated by that of the single ionization. If the ionization probability of per electron is constant in the same shell, the cross section of simultaneous single L and n-fold outer-shell ionization can be expressed by the binomial distribution.[34–36] Therefore, one can find that the multiple ionization degree is positive to the single ionization cross section. Single ionization produced by light ions is mainly induced by direct Coulomb collision. Such cross section is proportional to the square of the effective nuclear charge of incident ion.[25] As a result, the multiple ionization degree should be positively related to the effective nuclear charge.

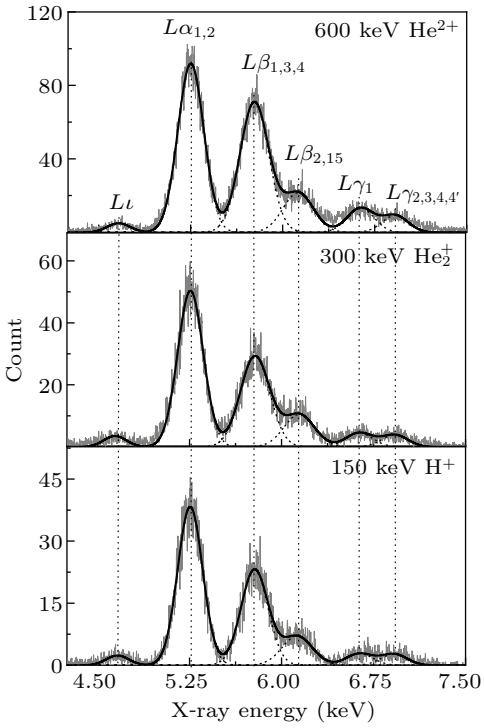


Fig. 5. The L x-ray spectra of neodymium induced by He^{2+}, H_2^+ and H^+ ions with the same single-nucleon energy.

As we all know, the effective nuclear charge of H^+ and He_2^+ are 1 and 2, respectively. By comparing the experimental and theoretical values of the potential function of hydrogen molecule-ion (H_2^+), the effective nuclear charge of H_2^+ is obtained of about 1.23, which is between that of H^+ and He_2^+.[37,38] As mentioned above, the outer-shell multiple ionization of Nd produced by H_2^+ ions impacting should be stronger than that by H^+ and weaker than that by He_2^+.

Figure 5 presents the Nd L-shell x-ray spectra produced by He^{2+}, H_2^+ and H^+ ions with the energy of 150 keV/u. It is obvious that the relative intensity of $L\beta_{2,15}$ x-ray is various for different incident ions, compared to the emission of $L\alpha_{1,2}$ x-ray. For further analysis, the relative intensity ratios of $L\beta_{1,3,4}$ and $L\beta_{2,15}$ to $L\alpha_{1,2}$ x-rays are extracted from the original counts. As shown in Figs. 6 and 7, the experimental results are larger than the theoretical value of single ionized atom and data of photon. In addition, this ratio increases as a function of effective nuclear charge. According to the effect of multiple ionization on the relative intensity ratio as discussed in Subsection 3.3, the present result confirms that the

multiple ionization of Nd produced by low energy light ions is positively correlated with the effective nuclear charge of the incident ion.

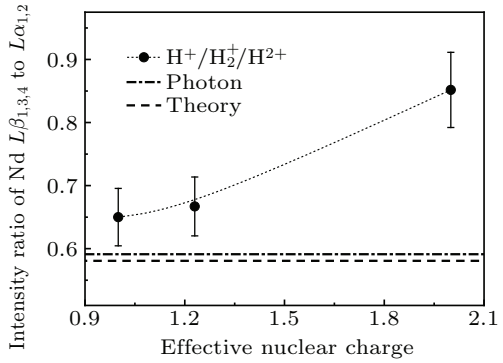


Fig. 6. Relative intensity ratios of Nd $L\beta_{1,3,4}$ to $L\alpha$ for H^+, H_2^+ and He^{2+} ions impact, and the data of photon and theoretical calculation for the singly ionized atom.

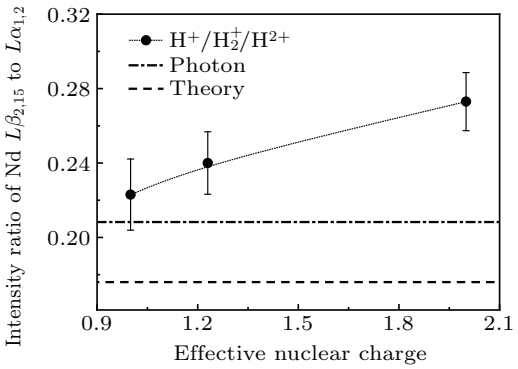


Fig. 7. Relative intensity ratios of Nd $L\beta_{2,15}$ to $L\alpha$ for H^+, H_2^+ and He^{2+} ions impact, and the data of photon and theoretical calculation for the singly ionized atom.

4. Conclusion

The Nd *L*-shell x-ray emission has been studied for the impact of 300–600 keV He^{2+} ions and H^+, H_2^+ ions with energy of 150 keV/u. It is indicated that there is a threshold for the Nd *L*-shell ionization in the energy region of 300–400 keV. The outer-shell electrons of Nd are multiply ionized by light ions, at the moment of *L* x-ray emission. This leads to a blue shift of the x-ray energy and an enhancement of the relative intensity ratios of the *L*-subshell x-rays. The extent of such multiple ionization is dwindled with increasing the incident energy and is enlarged as the projectile's effective nuclear charge increases.

Acknowledgements

The authors sincerely acknowledge the technical support from the group of 320 kV HCI platform.

Project supported by the National Key R&D Program of China (Grant No. 2017YFA0402300), the National Natural Science Foundation of China (Grant Nos. 11505248, 11775042, 11875096, and 11605147), the Scientific Research Program Funded by Shaanxi Provincial Education Department (Grant No. 20JK0975), Scientific Research Plan of Science and Technology Department of Shaanxi Province, China (Grant No. 2021JQ-812), Xianyang Normal University Science Foundation (Grant Nos. XSYK20024 and XSYK20009), and the academic leader of Xianyang Normal University (Grant No. XSYXSDT202108).

References

[1] Arnau A, Aumayr F, Echenique P M, Grether M, Heiland W, Limburg J, Morgenstern R, Roncin P, Schippers S, Schuch R, Stolterfoht N, Varga P, Zouros T J M and Winter H 1997 *Surf. Sci. Rep.* **27** 113
[2] Schenkel T, Hamza A V, Barnes A V and Schneider D H 1999 *Prog. Surf. Sci.* **61** 23
[3] Miranda J, Luciob O G and Lugo-Licona M F 2007 *Rev. Mex. Fis.* **53** 29
[4] Lapicki G 2019 *Nucl. Instrum. Methods B* **467** 123
[5] Zhou X M, Wei J, Cheng R, Zhao Y T, Zeng L X, Mei C X, Liang C H, Li Y Z, Zhang X A and Xiao G Q 2021 *Acta Phys. Sin.* **70** 023201 (in Chinese)
[6] Zhou X M, Wei J, Cheng R, Chen Y H, Mei C X, Zeng L X, Liang C H, Li Y Z, Zhao Y T and Zhang X A 2021 *Chin. Phys. B* **30** 083201
[7] Zhang X A, Mei C X, Zhang Y, Liang C H, Zhou X M, Zeng L X, Li Y Z, Liu Y, Xiang Q L, Meng H and Wang Y J 2020 *Acta Phys. Sin.* **69** 213301 (in Chinese)
[8] Liu Y, Xu Z F, Wang X, Zeng L X and Liu T 2020 *Acta Phys. Sin.* **69** 043201 (in Chinese)
[9] Ciricosta O, Vinkoe S M, Chung H K, Cho B I, Brown C R D, Burian T, Chalupsky J, Engelhorn K, Falcone RW, Graves C, Hájková V Higginbotham A, Juha L, Krzywinski J, Lee H J, Messerschmidt M, Murphy C D, Ping Y, Rackstraw D S, Scherz A, Schlotter W, Toleikis S, Turner J J, Vysin L, Wang T, Wu B, Zastrau U, Zhu D, Lee R W, Heimann P, Nagler B and Wark J S 2012 *Phys. Rev. Lett.* **109** 065002
[10] Szabo G L, Lehner M, Bischoff L, Pilz W, Muckenhuber H, Kentsch U, Aumayr F, Klingner N and Wilhelm R A 2021 *Nanotechnology* **32** 355701
[11] Wilhelm R A, Gruber E, Schwestka J, Kozubek R, Madeira T I Marques J P Kobus J, Krasheninnikov A V, Schleberger M and Aumayr F 2017 *Phys. Rev. Lett.* **119** 103401
[12] Garip A İ 1998 *Turk. J. Chem.* **22** 183
[13] Banaś D, Pajek M, Semaniak J, Braziewicz J, Kubala-Kukuś A, Majewska U, Czyżewski T, Jaskóła M, Kretschmer W, Mukoyama T and Trautmann D 2002 *Nucl. Instrum. Methods B* **195** 233
[14] Cipolla S J and Hill B P 2005 *Nucl. Instrum. Methods B* **241** 129
[15] Czarnota M, Banas D, Breset M, Chmielewska D, Dousse J C, Hoszowska J, Maillard Y P, Mauron O, Pajek M, Polasik M, Raboud P A, Rzadkiewicz J, Słabkowska K and Sujkowski Z 2010 *Eur. Phys. J. D* **57** 321
[16] Czarnota M, Pajek M, Banas D, Dousse J Cl, Maillard Y P, Mauron O, Raboud P A, Berset M, Chmielewska D, Rzadkiewicz J, Sujkowski Z, Hoszowska J, Slabkowska K and Polasik M 2006 *Braz. J. Phys.* **36** 546
[17] Lapicki G, Ramana Murty G A V, Naga Raju G J, Seetharami Reddy B, Bhuloka Reddy S and Vijayan V 2004 *Phys. Rev. A* **70** 062718
[18] Lapicki G, Mehta R, Duggan J L, Kocur P M, Price J L and McDanie F D 1986 *Phys. Rev. A* **34** 3813
[19] Miranda J, Lucio O G, Téllez E B, and Martínez J N 2004 *Radiat. Phys. Chem.* **69** 257
[20] Cipolla S J 2007 *Nucl. Instrum. Methods B* **261** 153
[21] Zhou X M, Wei J, Cheng R, Chen Y H, Zhao Y T and Zhang X A 2021 *Laser. Part. Beams.* **2021** 6653739
[22] Zhou X M, Zhao Y T, Cheng R, Wang Y Y, Lei Y and Wang X 2013 *Nucl. Instrum. Methods B* **299** 61
[23] Bearden J A 1967 *Rev. Mod. Phys.* **39** 78
[24] X-ray data book: http://xdb.lbl.gov/; Table of Isotopes: http://ie.lbl.gov/atom.htm
[25] McGuire J H and Richard P 1973 *Phys. Rev. A* **8** 1374
[26] Gryziński M 1965 *Phys. Rev.* **138** a336

[27] Zhao Y T, Xiao G Q, Zhang X A, Yang Z H, Zhang Y P, Chen X M, Zhang H Q, Cui Y, Shao J X, Xu X and Li F L 2005 *Int. J. Mod. Phys. B* **19** 2486

[28] Zhang X A, Li Y Z, Zhao Y T, Liang C H, Cheng R, Zhou X M, Wang X, Lei Y, Sun Y B, Xu G, Li J Y, Xiao G Q 2012 *Acta Phys. Sin.* **61** 113401 (in Chinese)

[29] Clementi E and Raimondl D L 1963 *J. Chem. phys.* **38** 2686

[30] Clementi E, Raimondi D L and Reinhardt W P 1967 *J. Chem. phys.* **47** 1300

[31] Zhou X M, Cheng R, Wang Y Y, Lei Y, Chen Y H, Chen X M, Zhao Y T and Xiao G Q 2017 *Nucl. Instrum. Methods B* **408** 140

[32] Krause M O 1979 *J. Phys. Chem. Ref. Data* **8** 307

[33] Crawford J, Cohen D, Doherty G and Atanacio A 2011 *Calculated K, L and M-shell X-ray Line Intensities for Light ion Impact on Selected Targets from Z = 6 to 100*, (Sydney: Australian Nuclear Science and Technology Organization)

[34] Kavčič M, Šmit Ž and Budnar M 1997 *Phys. Rev. A* **56** 4675

[35] Awaya Y, Kambara T and Kanai Y 1999 *Int. J. Mass. Spectrom.* **192** 49

[36] Czarnota M, Banaś D, Braziewicz J, Semaniak J, Pajek M, JaskółA M, Korman A, Trautmann D, Kretschmer W, Lapicki G and Mukoyama T 2009 *Phys. Rev. A* **79** 032710

[37] Lin J F 1999 *Journal of shanghai university if engineering science* **13** 140

[38] Qin A L and Guo Y C 2008 *Journal of Hebei university of engineering* (Natural Science Edition) **25** 100